Microfluidic ionic liquid dye laser

H. Zhang,† C. Zhang,† S. Vaziri, F. Kenarangi, Y. Sun*

Department of Electrical Engineering, University of Texas at Arlington, Arlington, TX 76019
†These authors contributed equally
*Corresponding author: sun@uta.edu

Abstract: In this work, by utilizing ionic liquid as the gain medium solvent, which is a new category of materials, we demonstrated a droplet-based dye laser system in a co-flowing microfluidic device. We characterized the droplet laser system and achieved a lasing threshold of 40.1 μJ/mm^2. Owning to the unique properties of ionic liquids, such as negligible vapor pressure and good thermal and chemical stability, they offer great potentials for the development of optofluidic lasers, tunable optofluidic devices, and sensitive biochemical analysis.

Index Terms: Ionic liquid, dye lasers, droplet lasers, microfluidics.

1. Introduction

Microfluidic dye lasers [1-3] use organic dyes as the gain medium, which are normally dissolved in a solvent, such as methanol, water or immersion oil. The broad fluorescence emission spectrum of the dye molecules (~30 nm) and the easy manipulation of different dye solutions enable a high tunability in terms of lasing emission. Depending on their molecular structures and polarities, organic dyes can be dissolved into either aqueous solvents [4-6] or oil-phase solvents [7-10]. However, the efforts to find certain universal solvents, which can dissolve both polar and non-polar organic dyes, is still ongoing. Ionic liquids (ILs) are the type of salts composed solely of ions in which some of them stay in the liquid state at room temperature [11]. ILs typically have excellent solubility for a large variety of organic chemicals. For example, Rhodamine 6G [12], a polar molecule, and Nile Red [13], a non-polar molecule, can both be dissolved in the ionic liquid [Bmim]PF6 with good quantum yields. The physical, chemical, and biological properties of ILs can be precisely adjusted for a wide range of utilization by varying the cations or anions and thus they have been generally recognized as designer solvents [14, 15]. Additionally, ILs have been acknowledged as the green solvents due to their non-volatility, low toxicity, nonflammability and high ionic conductivity. As a result, ILs have received significant interests as an environmentally friendly replacement to the traditional organic solvents [16].

A diverse variety of emerging applications of ILs in the field of microfluidics and optics have been witnessed over the past years, such as analytes extraction [17-19], new emulsion formation [20], and electro-optical modulation [21, 22]. Chen, et al. presented a localization of dyes at the water/IL interface and the absorption of dye into the IL phase through a sandwich liquid-core waveguide, which could be beneficial for monitoring dynamic extraction processes in biological research [17]. Wang, et al. generated water droplets in ILs via microfluidic chips and demonstrated a Rhodamine 6G extraction from water droplets to the bulk IL phase in only 0.51 seconds [18]. Wijethunga, et al. demonstrated drop-to-drop liquid-liquid microextraction based on electrowetting on dielectric (EWOD) digital microfluidic chip [19]. Kowacz, et al. reported that the spontaneous formation of nano-sized ionic liquid/water (IL/W) emulsion, providing a potential method for creating functional core-shell microcrystals [20]. Souza, et al. studied the optical nonlinearity of ILs and showed that the nonlinear refractive index and thermo-optical coefficient dispersion are determined by the anions of ILs, promoting the engineering of ILs to aim at optical nonlinear applications [23]. Li, et al. investigated the dynamic electrowetting and de-wetting of ILs on a hydrophobic surface. He, et al. designed an electric double-layer capacitor and reported that the electro-optical modulation amplitude and response speed were linked to the electrical conductivity and structures of ILs. These two demonstrations provide meaningful insights for the design and control of electro-optical imaging and communication systems [21, 22].

In terms of the development of laser systems, especially dye lasers, ILs can be a great alternative when compared with conventional organic solvents. The good thermal stability and almost-zero volatility of ILs allow laser systems to operate in a more temperature-tolerable environment. Their high solubility for both polar and non-polar dye molecules is essential to maintain high quantum yields and provides flexibility in the selection of various dyes to achieve a broadband lasing spectral coverage. With proper combination of different dyes, the study of fluorescence resonance energy transfer (FRET) within ILs has been explored [24], which shows the potential of developing ionic liquid dye lasers by utilizing FRET effects. Besides, the tunable chemical and biological properties of ILs appear to be attractive features in optofluidic laser intra-cavity sensing applications [2, 25, 26]. However, the potential of ILs in the development of liquid dye laser has largely been unexplored. So far, only random lasing was observed from different confinement geometries made of ILs, including an IL droplet of 2-mm in diameter freely suspended at the tip of a syringe needle in air [27]. In order to have a precisely controlled optical cavity, in this work, we employed a microfluidic device to generate IL droplets on-chip. The size of the IL droplets could be well controlled through predefined microfluidic channels and different flow rate profiles. The refractive index of the IL droplet was

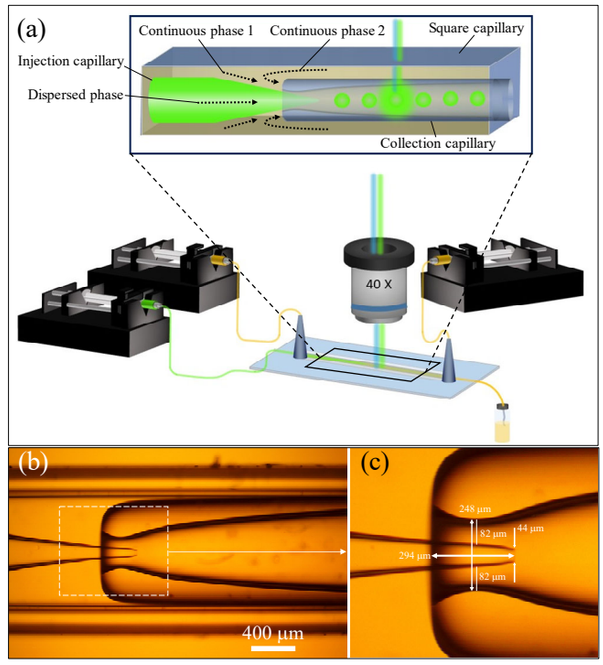

Fig. 1. (a) The schematic of the microcapillary device for droplet generation. Dispersed phase: ionic liquid [Bmim]PF6 with 1 v% Span 80; continuous phase 1 and 2 are 15.25 wt% PVA solution with 1 wt% SDS. (b) The optical image of the droplet generation site. (c) Zoom in view of the dash line region in (b) showing device dimensions.

chosen to be higher than that of the surrounding environment, thus through total internal reflection (TIR) light was confined within the surface of the droplets and formed whispering gallery modes (WGMs). Due to the interfacial tension between IL and the surrounding liquid, the surface of IL droplets was optically smooth, which minimizes the optical loss caused by scattering. Under pump lights, the WGMs interact with the gain molecules dissolved in the IL droplets. As the energy accumulates to reach the threshold, lasing emissions emerge from the droplets. In this work, we chose [Bmim]PF6 (1-Butyl-3-methylimidazolium hexafluorophosphate, refractive index n_{IL}=1.4085, viscosity 284.49 cP) as the IL for droplet generation and, for the first time to our knowledge, successfully demonstrated WGM lasing emission from dye-doped IL droplets in a microfluidic device.

2. Experimental Details

To obtain [Bmim]PF6 droplets, a co-flowing microfluidic device (inset of Fig. 1(a)) was fabricated through glass microcapillaries. The details of the fabrication process of the co-flowing microfluidic device was described elsewhere [28, 29]. As shown in Fig. 1, the square capillary (inner diameter ID 1.05 mm and outer diameter OD 1.3 mm) worked as a housing frame, then the injection capillary (ID 0.75 mm and OD 1 mm) and the collection capillary (ID 0.75 mm and OD 1 mm) were inserted into the square capillary from the opposite side, respectively. The tip of the injection capillary was tapered down to 44 μm. An orifice of 248 μm was created at the entrance of the collection capillary. Dispersed phase was driven through the injection capillary by a syringe pump. Continuous phase 1 was driven through the gap between injection capillary and square capillary, and continuous phase 2 was driven through the gap between the collection capillary and square capillary, by two other syringe pumps. To note that, the injection capillary was inserted into the orifice of the collection capillary, as shown in Fig. 1(b) and 1(c). The constrain from the orifice provides extra shear force and accelerates the breakup of IL droplets, resulting in a smaller diameter droplet. Dispersed phase was [Bmim]PF6 with 1 v% Span 80.

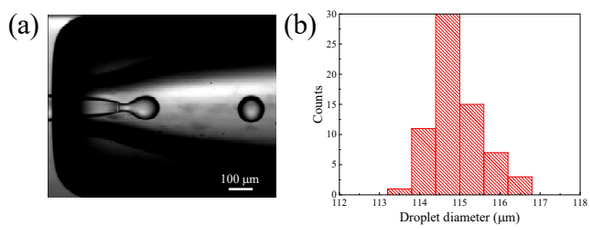

Fig. 2. (a) A snapshot of the generation of ionic liquid [Bmim]PF6 droplets. The flow rates of dispersed phase, continuous phase 1, and continuous phase 2 are 1 μL/hr, 600 μL/hr, and 200 μL/hr, respectively. (b) The size distribution of [Bmim]PF6 droplets.

Both continuous phase 1 and continuous phase 2 were 15.25 wt% PVA (polyvinyl alcohol, MW 13,000~23,000) solution with 1 wt% SDS (sodium dodecyl sulfate) surfactant. The main purpose of the continuous phase 2 was to fill up the gaps between the collection capillary and the square capillary to maintain a stable flow profile within the microfluidic channels. PVA solutions from continuous phase 1 and 2 were driven to pass through the orifice. Due to the shear stress exerted on the interface between IL and PVA solution, IL droplets grew and got pinched off from the tip of the injection capillary. The optical images of generated droplets were taken by a high-speed camera (Fastec IL5), as shown in Fig. 2(a). The flow rate profile of dispersed phase (Q_d) and continuous phases 1 (Q_{c1}) and 2 (Q_{c1}) was 1 μL/hr, 600 μL/hr and 200 μL/hr, respectively. Droplet diameter was measured by the droplet morphometry and velocimetry (DMV) program [30]. The size distribution of IL droplets is shown in Fig. 2(b). The average droplet diameter is 114.8±0.5 μm. To compare the measured droplet size with a simple scaling model, the droplet size can be predicted by finding the roots of a nondimensional equation derived by Umbanhowar et al [31]. Furthermore, when the dispersed phase is slow enough (in our case $Q_d/Q_{c1+c2}=1/800$), the predicted droplet size is

$$đ \approx 1+1/3Ca \quad (1)$$

in which, $đ=d/d_i$ is the droplet size (represented by d) scaled by the inner diameter (represented by d_i) of the tip of the injection capillary. $Ca \equiv \mu_c Q_c/\sigma A_c$ is the capillary number. A_c is denoting the cross-sectional area of the outer channel, which is the ring area between the orifice and the injection capillary. Q_c is the flow rate of continuous phase (the sum of continuous phase 1 and 2, $Q_c=Q_{c1}+Q_{c2}$), 800 μL/hr. μ_c is the viscosity of continuous phase, which is 205 mPa.s for 15.25 wt% PVA solution (value extracted from Ref. [32]). σ is the interfacial tension between dispersed phase and continuous phase, which is 5.6 mN/m. The measurement was performed using the pendant droplet method [33]. After inserting all the parameters into Eqn. (1), the predicted droplet size is 121 μm, which is very close to the measured droplet size.

3. Results

To confine the light within an IL droplet, the refractive index of the droplet should be higher than that of the surrounding environment to meet the condition of TIR, so that the WGMs can be supported. For this purpose, we have selected [Bmim]PF6 (refractive index $n_{IL}=1.41$) to form the droplet and 15.25 wt% PVA solution (refractive index $n_{PVA}=1.36$) as the surrounding liquid. The gain medium, organic dye BODIPY (1,3,5,7–Tetramethyl–8-phenyl-4,4-difluoroboradiazaindacene) was firstly dissolved into chloroform with a concentration of 50 mM. Then at a volume ratio of 1:100, BODIPY in chloroform solution was mixed with [Bmim]PF6, resulting in a 500 μM BODIPY in [Bmim]PF6 after the evaporation of chloroform at room temperature. The fluorescent spectrum of BODIPY in [Bmim]PF6 solution was recorded, as shown in Fig. 3(a). An OPO pulsed laser (excitation wavelength 485 nm, repetition rate 2 Hz) was used as the excitation source. The details of the experimental setup was described elsewhere [7, 34]. With the previously mentioned flow rate profile for dispersed phase and continuous phases (Q_d=1 μL/hr, Q_{c1}=600 μL/hr and Q_{c2}=200 μL/hr), BODIPY doped [Bmim]PF6 droplets were generated and flowing down the microfluidic device. While the moving droplets were excited under the pump beam, the emission spectra from them were recorded. When the pump energy exceeded the lasing threshold, WGM lasing emission was observed from the IL droplets and an example of the corresponding emission spectrum is presented in Fig. 3(b). The central wavelength of the lasing emission emerged at around 527 nm while the peak intensity of the fluorescence was around 518 nm. In general, the wavelength of lasing peaks is on the longer wavelength side of the fluorescent spectrum, where the gain is higher than the loss within the droplet ring resonator.

Since the [Bmim]PF6 droplets were excited while they were still moving inside the microfluidic channel, different spatial location of each droplet to the center of the pump beam spot would affect the coupling efficiency of pump light. The size of the pump beam spot was around 600 μm in diameter. As shown in Fig. 4(a), when an IL droplet is flowing by the excitation laser beam spot, their optical images (1 - 7) presented different brightness, indicating different fluorescent or lasing emission intensity from the droplet. Meanwhile, the emission spectrum from each droplet was simultaneously recorded by a spectrometer, as shown in Fig. 4(b). When droplets were outside of the pump beam area, they did not receive pump energy high enough to sustain lasing, such as Spectrum 1, 2, 6, and 7 in Fig. 4(b). When droplets have a good overlap with the pump beam, lasing emission emerged, such as Spectrum 3-5. Especially, droplets that were near the center of the pump

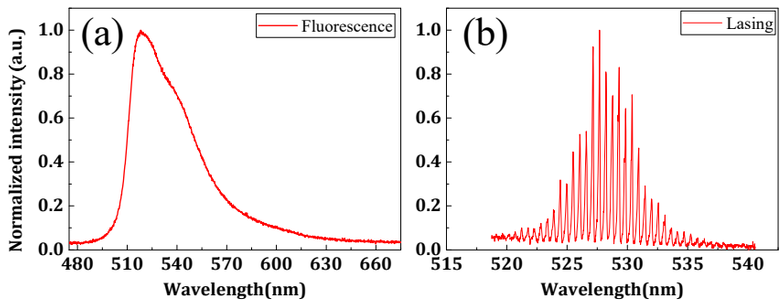

Fig. 3. (a) The fluorescence spectrum of 500 μM BODIPY in [Bmim]PF6. (b) The lasing spectrum from a [Bmim]PF6 droplet doped with 500 μM BODIPY.

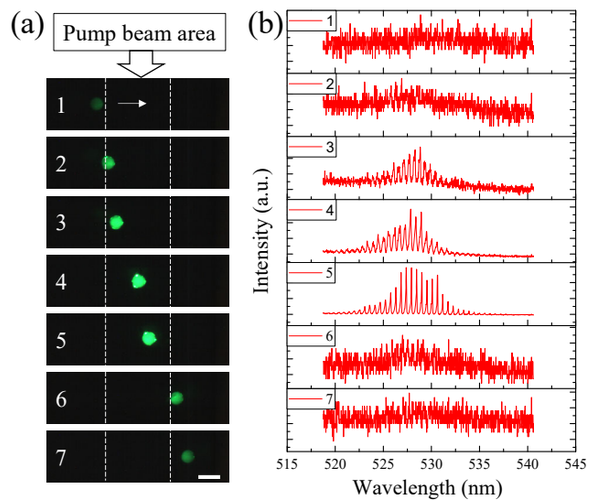

Fig. 4. (a) Images of [Bmim]PF6 droplets flowing by the excitation laser beam spot. The arrow indicates flow direction. Dashed lines outline the area of excitation laser beam spot. The scale bar is 200 μm. (b) The corresponding spectra collected from the [Bmim]PF6 droplets in (a).

beam got excited most efficiently, represented by Spectrum 4 and 5. The free spectral range (FSR) measured from the lasing spectra is 0.542 nm. The droplet size can be calculated using equation, $\Delta\lambda=\lambda^2/(\pi nd)$, in which, λ is the central wavelength of the lasing spectrum (λ = 527 nm), $\Delta\lambda$ is the FSR, n is the effective refractive index of the WGMs ($n \approx 1.41$), and d is the diameter of droplets. The calculated droplet size is 115 μm, which is consistent with the measurement of the droplet size acquired in the microscope images in Fig. 4(a). This confirms the WGM nature of the lasing emission, which is from the droplet cavity. Although the collection capillary top and bottom surfaces form a Fabry–Pérot (FP) cavity which may support lasing when IL droplets are present, the measured FSR does not match the size of the FP cavity.

To study the lasing threshold of BODIPY-doped [Bmim]PF6 droplets, different excitation power densities were applied to the droplet and the emission spectra from the droplet were simultaneously recorded. As shown in Fig. 5(a), at pump power below the lasing threshold, no lasing emission was observed. When the pump power crossed the lasing threshold, sharp lasing peaks started to emerge. The intensity of the lasing emission increased proportionally to the increase of the pump power density above the lasing threshold. The integrated emission intensity was plotted in Fig. 5(b) at different pump power densities. The linear fitting of the datapoints in the lasing region revealed a lasing threshold of 40.1 μJ/mm^2. This lasing

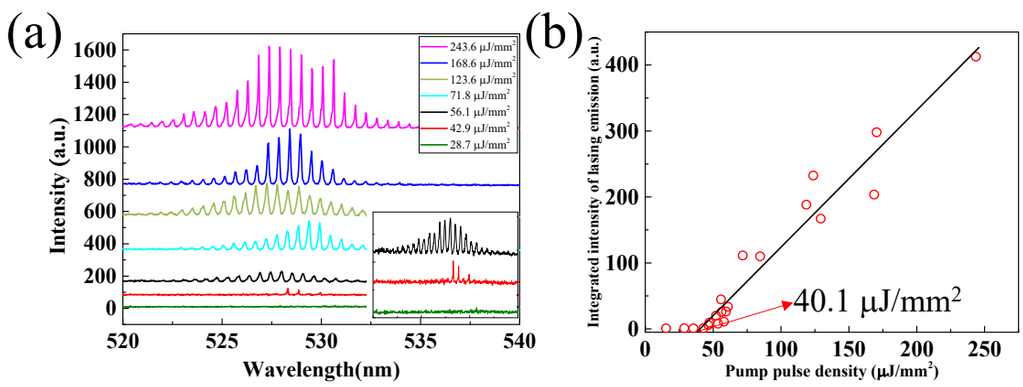

Fig. 5. (a) The emission spectra of [Bmim]PF6 droplets under different pump density at the same pump location. The inset shows a zoom-in view of the bottom three spectra. (b) The dependence of integrated lasing emission intensity on pump pulse density. The lasing threshold is 40.1 μJ/mm^2.

threshold is a few times higher than that of demonstrated in several other optofluidic droplet lasers [5, 7, 8, 35-37]. One reason contributed to a higher lasing threshold is the small refractive index difference (which is 0.05) between [Bmim]PF6 and the PVA solution. The intrinsic cavity Q factor of the droplet was compromised by the radiative loss of the droplet itself, thus the light confinement became weaker and a higher pump energy was needed to achieve lasing. However, this is not an intrinsic limitation of an IL droplet laser. By choosing different material combinations for the droplet cavity and its surrounding liquid, a higher refractive index difference can be readily achieved, and thus an IL droplet laser system with low lasing threshold would be within reach.

4. Conclusions

In conclusion, we have successfully demonstrated IL droplet microlasers through a co-flowing microfluidic device. By reducing the diameter of the orifice, the shear force around the injection tip increases, which helps IL droplets to break off easier even when the continuous phase has a low viscosity. Thus, using water instead of PVA solution becomes feasible, which would contribute to a more efficient laser system with a lower lasing threshold. In this work, the [Bmim]PF6 was chosen as an example for the demonstration of IL droplet lasing. However, there are hundreds of types of ILs. Some of them like [Bmim]PF6 could be a great replacement for the flammable and volatile conventional organic solvents for the development of microlasers and liquid lasers. The diverse physical, chemical, and biological properties of ILs open new opportunities in liquid lasers and laser-based bio/chemical sensors. Our laser system can be easily transferred to Si/PDMS-based microfluidic networks for integrated on-chip light sources and high-throughput microanalysis development.

Funding sources.

This work was supported by the National Science Foundation (1554013).

Disclosures.

The authors declare no conflicts of interest.

References

[1] Z. Li and D. Psaltis, "Optofluidic dye lasers," *Microfluid Nanofluidics,* vol. 4, no. 1-2, pp. 145-158, Jan. 2008.

[2] X. Fan and S. H. Yun, "The potential of optofluidic biolasers," *Nat. Methods,* vol. 11, no. 2, pp. 141-147, Jan. 2014.

[3] H. Schmidt and A. R. Hawkins, "The photonic integration of non-solid media using optofluidics," *Nat. Photonics,* vol. 5, no. 10, pp. 598-604, Aug. 2011.

[4] M. Tanyeri, R. Perron, and I. M. Kennedy, "Lasing droplets in a microfabricated channel," *Opt. Lett.,* vol. 32, no. 17, pp. 2529-2531, Jan. 2007.

[5] L. Zheng, M. Zhi, Y. Chan, and S. A. Khan, "Embedding liquid lasers within or around aqueous microfluidic droplets," *Lab Chip,* vol. 18, no. 1, pp. 197-205, Jan. 2018.

[6] L. Labrador-Páez, K. Soler-Carracedo, M. Hernández-Rodríguez, I. R. Martín, T. Carmon, and L. L. Martin, "Liquid whispering-gallery-mode resonator as a humidity sensor," *Opt. Express,* vol. 25, no. 2, pp. 1165-1172, Jan. 2017.

[7] H. Zhang and Y. Sun, "Optofluidic droplet dye laser generated by microfluidic nozzles," *Opt. Express,* vol. 26, no. 9, pp. 11284-11291, Apr. 2018.

[8] M. Humar and S. H. Yun, "Intracellular microlasers," *Nat. Photonics,* vol. 9, no. 9, pp. 572-576, Jul. 2015.

[9] M. Aas, A. Jonáš, and A. Kiraz, "Lasing in optically manipulated, dye-doped emulsion microdroplets," *Opt. Commun.,* vol. 290, pp. 183-187, Mar. 2013.

[10] H. Zhang, P. Palit, Y. Liu, S. Vaziri, and Y. Sun, "Reconfigurable Integrated Optofluidic Droplet Laser Arrays," *ACS Appl. Mater. Interfaces,* vol. 12, no. 24, pp. 26936-26942, May 2020.

[11] S. Sowmiah, V. Srinivasadesikan, M. Tseng, and Y. Chu, "On the chemical stabilities of ionic liquids," *Molecules,* vol. 14, no. 9, pp. 3780-3813, Sep. 2009.

[12] J. H. Werner, S. N. Baker, and G. A. Baker, "Fluorescence correlation spectroscopic studies of diffusion within the ionic liquid 1-butyl-3-methylimidazolium hexafluorophosphate," *Analyst,* vol. 128, no. 6, pp. 786-789, Apr. 2003.

[13] K. A. Fletcher, I. A. Storey, A. E. Hendricks, S. Pandey, and S. Pandey, "Behavior of the solvatochromic probes Reichardt's dye, pyrene, dansylamide, Nile Red and 1-pyrenecarbaldehyde within the room-temperature ionic liquid bmimPF6," *Green Chem.,* vol. 3, no. 5, pp. 210-215, Aug. 2001.

[14] R. D. Rogers and K. R. Seddon, "Ionic liquids--solvents of the future?," *Science,* vol. 302, no. 5646, pp. 792-793, Oct. 2003.

[15] E. F. Borra, O. Seddiki, R. Angel, D. Eisenstein, P. Hickson, K. R. Seddon, and S. P. Worden, "Deposition of metal films on an ionic liquid as a basis for a lunar telescope," *Nature,* vol. 447, no. 7147, pp. 979-981, Jun. 2007.
[16] S. Mallakpour and Z. Rafiee, "Ionic liquids as environmentally friendly solvents in macromolecules chemistry and technology, Part I," *J. Polym. Environ.,* vol. 19, no. 2, pp. 447-484, Mar. 2011.
[17] X. Chen, A. Sakurazawa, K. Sato, K.-I. Tsunoda, and J. Wang, "A Solid-Cladding/Liquid-Core/Liquid-Cladding Sandwich Optical Waveguide for the Study of Dynamic Extraction of Dye by Ionic Liquid BmimPF6," *Appl. Spectrosc.,* vol. 66, no. 7, pp. 798-802, Jul. 2012.
[18] W. Wang, Z. Zhang, Y. Xie, L. Wang, S. Yi, K. Liu, J. Liu, D. Pang, and X. Zhao, "Flow-focusing generation of monodisperse water droplets wrapped by ionic liquid on microfluidic chips: From plug to sphere," *Langmuir,* vol. 23, no. 23, pp. 11924-11931, Oct. 2007.
[19] P. A. Wijethunga, Y. S. Nanayakkara, P. Kunchala, D. W. Armstrong, and H. Moon, "On-chip drop-to-drop liquid microextraction coupled with real-time concentration monitoring technique," *Anal. Chem.,* vol. 83, no. 5, pp. 1658-1664, Feb. 2011.
[20] M. Kowacz, J. M. Esperança, and L. P. N. Rebelo, "Spontaneous emulsification in ionic liquid/water systems and its use for templating of solids," *Soft Matter,* vol. 10, no. 21, pp. 3798-3805, Feb. 2014.
[21] X. He, Q. Shao, P. Cao, W. Kong, J. Sun, X. Zhang, and Y. Deng, "Electro-optical phenomena based on ionic liquids in an optofluidic waveguide," *Lab Chip,* vol. 15, no. 5, pp. 1311-1319, Jan. 2015.
[22] H. Li, M. Paneru, R. Sedev, and J. Ralston, "Dynamic electrowetting and dewetting of ionic liquids at a hydrophobic solid–liquid interface," *Langmuir,* vol. 29, no. 8, pp. 2631-2639, Jan. 2013.
[23] R. Souza, M. Alencar, M. Meneghetti, J. Dupont, and J. Hickmann, "Nonlocal optical nonlinearity of ionic liquids," *J. Phys. Condens. Matter,* vol. 20, no. 15, p. 155102, Mar. 2008.
[24] H. Izawa, S. Wakizono, and J.-i. Kadokawa, "Fluorescence resonance-energy-transfer in systems of Rhodamine 6G with ionic liquid showing emissions by excitation at wide wavelength areas," *Chem. Commun.,* vol. 46, no. 34, pp. 6359-6361, Aug. 2010.
[25] Y. Sun and X. Fan, "Distinguishing DNA by Analog-to-Digital-like Conversion by Using Optofluidic Lasers," *Angew. Chem.,* vol. 51, no. 5, pp. 1236-1239, Jan. 2012.
[26] X. Wu, M. K. K. Oo, K. Reddy, Q. Chen, Y. Sun, and X. Fan, "Optofluidic laser for dual-mode sensitive biomolecular detection with a large dynamic range," *Nat. Commun.,* vol. 5, no. 1, p. 3779, Apr. 2014.
[27] V. Barna and L. De Cola, "Mirrorless dye doped ionic liquid lasers," *Opt. Express,* vol. 23, no. 9, pp. 11936-11945, May 2015.
[28] A. S. Utada, E. Lorenceau, D. R. Link, P. D. Kaplan, H. A. Stone, and D. Weitz, "Monodisperse double emulsions generated from a microcapillary device," *Science,* vol. 308, no. 5721, pp. 537-541, Apr. 2005.
[29] H. Zhang, C. Zhang, and Y. Sun, "Double emulsion optofluidic microlasers," in *Frontiers in Biological Detection: From Nanosensors to Systems XI*, Mar. 2019, vol. 10895: International Society for Optics and Photonics.
[30] A. S. Basu, "Droplet morphometry and velocimetry (DMV): a video processing software for time-resolved, label-free tracking of droplet parameters," *Lab Chip,* vol. 13, no. 10, pp. 1892-1901, Mar. 2013.
[31] P. Umbanhowar, V. Prasad, and D. A. Weitz, "Monodisperse emulsion generation via drop break off in a coflowing stream," *Langmuir,* vol. 16, no. 2, pp. 347-351, Jan. 2000.
[32] A. Norton, R. Hancocks, and L. Grover, "Poly (vinyl alcohol) modification of low acyl gellan hydrogels for applications in tissue regeneration," *Food Hydrocoll.,* vol. 42, pp. 373-377, Dec. 2014.

[33] J. D. Berry, M. J. Neeson, R. R. Dagastine, D. Y. Chan, and R. F. Tabor, "Measurement of surface and interfacial tension using pendant drop tensiometry," *J. Colloid Interface Sci.,* vol. 454, pp. 226-237, Sep. 2015.
[34] H. Zhang, A. Balram, D. D. Meng, and Y. Sun, "Optofluidic lasers with monolayer gain at the liquid–liquid interface," *ACS Photonics,* vol. 4, no. 3, pp. 621-625, Feb. 2017.
[35] R. Chen and H. D. Sun, "Tuning whispering gallery mode lasing from self-assembled polymer droplets," *Sci. Rep.,* vol. 3, no. 1, pp. 1-5, Mar. 2013.
[36] S. K. Tang, Z. Li, A. R. Abate, J. J. Agresti, D. A. Weitz, D. Psaltis, and G. M. Whitesides, "A multi-color fast-switching microfluidic droplet dye laser," *Lab Chip,* vol. 9, no. 19, pp. 2767-2771, Aug. 2009.
[37] S. K. Tang, R. Derda, Q. Quan, M. Lončar, and G. M. Whitesides, "Continuously tunable microdroplet-laser in a microfluidic channel," *Opt. Express,* vol. 19, no. 3, pp. 2204-2215, Jan. 2011.